

Redox and photochemical behaviour of a porphyrin monolayer on an indium-tin oxide electrode

Naoko Araki^{a,*}, Makoto Obata^a, Akio Ichimura^b, Yutaka Amao^c,
Kazunori Mitsuo^d, Keisuke Asai^e, Shigenobu Yano^{a,*}

^a Division of Natural Science and Ecological Awareness, Graduate School of Humanities and Sciences, Nara Women's University, Kita-uoya-nishi-machi, Nara-shi 630-8506, Japan

^b Department of Chemistry, Graduate School of Science, Osaka City University, 3-3-138 Sugimoto, Sumiyoshi-ku, Osaka 558-8585, Japan

^c Department of Applied Chemistry, Oita University, Dannoharu 700, Oita 870-1192, Japan

^d Aerodynamics Research Group, Institute of Space Technology and Aeronautics, Japan Aerospace Exploration Agency, 7-44-1, Jindaiji Higashi Chofu City, Tokyo 182-8522, Japan

^e Department of Aeronautics and Space Engineering, Tohoku University, 01 Aoba, Aoba-ku, Sendai 980-8579, Japan

Received 13 January 2005; received in revised form 19 April 2005; accepted 15 May 2005

Available online 5 July 2005

Abstract

In order to investigate photoluminescence behaviour of an ordered molecular porphyrin monolayer and its quenching properties by oxygen gas, a porphyrin with long alkyl chains, 5,10,15,20-tetrakis[4-(11-carboxylundecane-1-oxy)phenyl]porphyrin (**4**), was synthesized and adsorbed onto an indium-tin oxide (ITO) substrate by a chemical dipping method. Cyclic voltammetry was used to analyze the ITO electrode coated with **4**. The peak current of the first oxidation was proportional to the sweep rate, and the surface coverage was estimated to be $2.3\text{--}2.5 \times 10^{-10} \text{ mol cm}^{-2}$. The UV–vis spectrum of the monolayer showed a broadened Soret band, which shifted to longer wavelength. These features suggest that the porphyrin moieties of **4** are packed to form a *J*-type structure. The oxygen quenching ratio of the porphyrin **4** monolayer on the ITO electrode, I_0/I_{100} , was estimated to be 1.25, where I_0 and I_{100} are, respectively, luminescence intensity values in 100% argon and 100% oxygen. On repeated step cycling between 100% argon and 100% oxygen atmospheres, the response times of luminescence quenching were 10 s (argon to oxygen) and 23 s (oxygen to argon). These findings suggest that a monolayer of sensing dye is applicable for oxygen sensing system without deterioration of size-accuracy of models.

© 2005 Elsevier Ltd. All rights reserved.

Keywords: Porphyrin monolayer; Oxygen quenching; Photochemistry; Indium-tin oxide; Cyclic voltammetry

1. Introduction

Self-assembled monolayers (SAMs) have emerged as an alternative and useful strategy for assembling molecular components on surface. SAMs have been used to develop novel surface-patterning methodologies, to fabricate new types of chemically sensitive devices, to study interfacial electron transfer processes and to prepare a variety of unusual and potentially useful electronic, photonic and redox-active mate-

rials [1,2]. Porphyrins on gold surfaces using S–Au linkages have been widely studied for application to molecular devices. One reason for this interest is the porphyrin's large molar absorption coefficient in the visible light region. Another reason is efficient electron transfer from the excited state of porphyrin to ground state of various acceptors and donors such as ferrocene and fullerene derivatives [3–7]. Furthermore, the oxygen-induced luminescence quenching properties have been examined for thin films consisting of porphyrins, such as polymer films, Langmuir–Blodgett (LB) films and chemisorption films [8–12]. However, the photoluminescence behaviour and its quenching properties by oxygen gas remain to be fully understood for ordered molecular

* Corresponding authors. Tel.: +81 742 20 3392; fax: +81 742 20 3392.

E-mail addresses: xan.araki@cc.nara-wu.ac.jp (N. Araki), yano@cc.nara-wu.ac.jp (S. Yano).

porphyrin SAMs. In this study, we focused on the photoluminescence behaviour of a porphyrin SAMs. While the most established SAM system is alkanethiols on gold surfaces [13,14], a strong quenching of the porphyrin excited singlet state by the gold surface enhances non-radiative losses. Indium-tin oxide (ITO) is a promising candidate as a substrate for photoluminescence study because the ITO electrode has high optical transmission and suppresses the quenching of the porphyrin excited states [13]. Therefore, we investigated photoluminescence behaviour of porphyrin SAM on an ITO electrode and its quenching properties by oxygen gas.

Spontaneous adsorption of long-chain *n*-alkanoic acid ($C_nH_{2n+1}COOH$) on AgO, Al₂O₃ and gold surfaces, has been studied in the past few years [15–18]. However, we are not aware of any studies on stable porphyrin SAMs formed from *n*-alkanoic acids on an ITO surface. We report, herein the synthesis of a functionalized porphyrin derivative, namely 5,10,15,20-tetrakis[4-(11-carboxylundecane-1-oxy)phenyl]porphyrin, and the preparation of a self-assembled monolayer of the porphyrin on an ITO electrode. The monolayer on the electrode was characterized by cyclic voltammetry and UV–vis absorption spectroscopy. The photoluminescence behaviour of the porphyrin monolayer and its quenching property by oxygen gas are discussed on the basis of luminescence measurements in the presence of argon and oxygen gases.

2. Experimental

2.1. Materials

All solvents and chemicals were of reagent grade quality obtained from Wako Pure Chemical Industries Ltd., Osaka, Japan, and were used without further purification unless otherwise noted. The solvents for cyclic voltammetry were passed through a short alumina column just before use. Tetrabutylammonium hexafluorophosphate (Bu₄NPF₆) was obtained from Tokyo Kasei Kogyo Co. Ltd., Tokyo, Japan, and recrystallized from EtOH just before use.

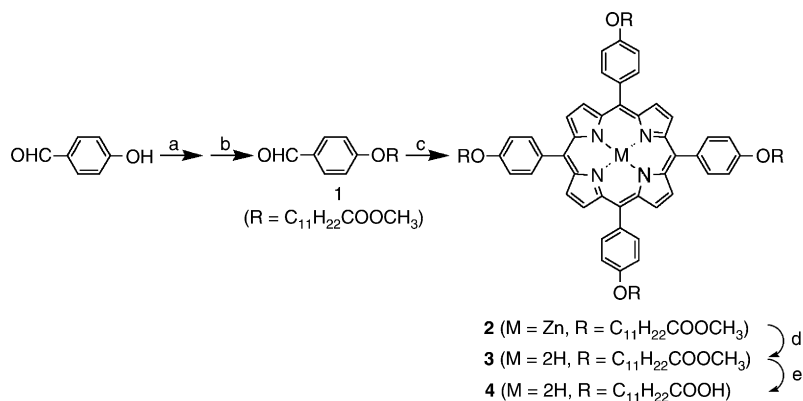
2.2. Synthesis

2.2.1. General

Porphyrin derivative **4** was prepared according to Scheme 1. ¹H NMR spectra were recorded on a Varian Gemini 2000 (300 MHz) instrument. Fast atom bombardment mass spectra (FAB-MS) were measured on a JMS-700T spectrometer (Osaka City University) using 3-nitrobenzyl alcohol as a matrix. Elemental analysis was carried out using a Perkin-Elmer 240C Elemental Analyzer (Osaka City University).

2.2.2. Methyl 12-(4-formylphenoxy)dodecanate (**1**)

A solution of *p*-hydroxybenzaldehyde (6.07 g, 49.7 mmol) in 5% NaOH (aq) (70 mL) was vigorously stirred at room temperature with CH₂Cl₂ (50 mL) and tetrabutylammonium bromide (3.07 g, 9.52 mmol). To the mixture was added a solution of 12-bromododecanoic acid (2.34 g, 8.38 mmol) in CH₂Cl₂ (20 mL) and the whole was stirred at room temperature for 60 h. The organic layer was washed with 5% NaOH (aq) and water, and then dried over Na₂SO₄, and the solvent was removed under reduced pressure. The residue was reprecipitated from hot MeOH to afford crude 12-(4-formylphenoxy)dodecanoic acid as a white powder (1.80 g). The crude product (5.82 g) was taken up in a mixture of MeOH (500 mL) and benzene (100 mL). Hydrogen chloride gas was introduced into the mixture for 2 h, and then the mixture was refluxed at 90–95 °C for 3 days with azeotropic distillation of water. After cooling, the mixture was poured into water and extracted with CHCl₃. The organic layer was washed with saturated NaHCO₃ (aq) and water, dried over Na₂SO₄, and evaporated. The residue was purified by silica gel column chromatography with ethyl acetate/hexane (5/12, v/v) as an eluent (*R*_f = 0.58), followed by precipitation from hot hexane to afford methyl 12-(4-formylphenoxy)dodecanate (**1**) as a white solid (1.39 g, 4.37 mmol, 19.1%). ¹H NMR (300 MHz, CDCl₃): δ 9.88 (s, 1H, –CHO), 7.81 (d, ³*J* = 8.85 Hz, 2H, ArH), 6.98 (d, ³*J* = 8.54 Hz, 2H, ArH), 4.03 (t, ³*J* = 6.68 Hz, 2H, –OCH₂–),



Scheme 1. Reagents and conditions: (a) 12-bromododecanoic acid, Bu₄NBr, 5 wt% NaOH (aq), CH₂Cl₂, r.t., (b) MeOH, HCl (gas), benzene, reflux, (c) pyrrole, Zn(OAc)₂·2H₂O, BF₃·OEt₂, CHCl₃, *p*-chloranil, (d) 6 M HCl and (e) KOH, MeOH, THF.

3.66 (s, 3H, $-\text{COOCH}_3$), 2.28 (t, $^3J=7.63$ Hz, 2H, $-\text{CH}_2\text{COOCH}_3$), 1.85–1.28 (m, 18H, $-\text{OCH}_2(\text{CH}_2)_9-$).

2.2.3. 5,10,15,20-Tetrakis[4-(11-methoxycarbonylundecane-1-oxy)phenyl]porphyrinato zinc(II) (**2**)

Pyrrole (0.3 mL, 4.36 mmol), **1** (1.01 g, 3.03 mmol) and $\text{Zn}(\text{OAc})_2 \cdot 2\text{H}_2\text{O}$ (2.7 g, 12.3 mmol) were added to CHCl_3 (300 mL) that had been purged with argon for 30 min. $\text{BF}_3 \cdot \text{OEt}_2$ (0.2 mL, 1.60 mmol) was added to the mixture to initiate the reaction. After introduction of additional argon gas for 10 min, the mixture was stirred at 30 °C for 3.5 h, and then *p*-chloranil (0.56 g, 2.27 mmol) was added. The mixture was refluxed for 1 h, washed with saturated NaHCO_3 (aq) and water, and dried over Na_2SO_4 . Silica gel (5 g) was added to the dark solution, and all solvents were removed by evaporation. The silica gel containing the absorbed products was placed on top of a silica gel column and elution was carried out with a mixture of $\text{CH}_2\text{Cl}_2/\text{acetone}$ (12/1, v/v). The red band ($R_f=0.79$) was collected. Evaporation of the solvent and precipitation from $\text{CH}_2\text{Cl}_2/\text{MeOH}$ afforded 5,10,15,20-tetrakis[4-(11-methoxycarbonylundecane-1-oxy)phenyl]porphyrinato zinc(II) (**2**) as a purple solid (0.41 g, 0.26 mmol, 34.7%). ^1H NMR (300 MHz, CDCl_3): δ 8.97 (s, 8H, pyrrole- βH), 8.09 (d, $^3J=8.54$ Hz, 8H, ArH), 7.25 (d, $^3J=8.85$ Hz, 8H, ArH), 4.24 (t, $^3J=6.41$ Hz, 8H, $-\text{OCH}_2-$), 3.65 (s, 12H, $-\text{COOCH}_3$), 2.28 (t, $^3J=7.33$ Hz, 8H, $-\text{CH}_2\text{COOCH}_3$), 2.01–1.34 (m, 72H, $-\text{OCH}_2(\text{CH}_2)_9-$). FAB-MS for $\text{Zn}_1\text{C}_{96}\text{H}_{124}\text{O}_{12}\text{N}_4$: m/z calcd., 1591.4 [M] $^+$: found, 1590.9.

2.2.4. 5,10,15,20-Tetrakis[4-(11-methoxycarbonylundecane-1-oxy)phenyl]porphyrin (**3**)

A solution of **2** (0.36 g, 0.23 mmol) in CH_2Cl_2 (50 mL) was washed several times with 6 M HCl (aq), saturated NaHCO_3 (aq) and dried over Na_2SO_4 . Evaporation of the solvent and precipitation from $\text{CH}_2\text{Cl}_2/\text{MeOH}$ gave 5,10,15,20-tetrakis[4-(11-methoxycarbonylundecane-1-oxy)phenyl]porphyrin (**3**) as a purple solid (0.32 g, 0.21 mmol, 92.6%). ^1H NMR (300 MHz, CDCl_3): δ 8.86 (s, 8H, pyrrole- βH), 8.09 (d, $^3J=8.54$ Hz, 8H, ArH), 7.25 (d, $^3J=8.85$ Hz, 8H, ArH), 4.24 (t, $^3J=6.41$ Hz, 8H, $-\text{OCH}_2-$), 3.67 (s, 12H, $-\text{COOCH}_3$), 2.30 (t, $^3J=7.63$ Hz, 8H, $-\text{CH}_2\text{COOCH}_3$), 2.00–1.34 (m, 72H, $-\text{OCH}_2(\text{CH}_2)_9-$), -2.66 (s, 2H, -2NH). FAB-MS for $\text{C}_{96}\text{H}_{126}\text{O}_{12}\text{N}_4$: m/z calcd., 1529.0 [$M + \text{H}$] $^+$: found, 1529.0.

2.2.5. 5,10,15,20-Tetrakis[4-(11-carboxylundecane-1-oxy)phenyl]porphyrin (**4**)

Porphyrin **3** (0.72 g, 0.45 mmol) was dissolved in THF (150 mL) and stirred at room temperature. To this stirred mixture was added a solution prepared by mixing MeOH (150 mL) and KOH (5.26 g, 93.7 mmol). The solution was stirred at room temperature for 24 h, and then acidified with 1 M HCl (aq) to adjust the pH to 4. Then the reaction mixture was diluted with water (1 L) and

subsequent filtration resulted in 5,10,15,20-tetrakis[4-(11-carboxylundecane-1-oxy)phenyl]porphyrin (**4**) as a purple solid (0.69 g, 0.44 mmol, 97.3%). ^1H NMR (300 MHz, THF-d_8): δ 8.83 (s, 8H, pyrrole- βH), 8.05 (d, $^3J=8.54$ Hz, 8H, ArH), 7.27 (d, $^3J=8.85$ Hz, 8H, ArH), 4.20 (t, $^3J=6.41$ Hz, 8H, $-\text{OCH}_2-$), 2.20 (t, $^3J=7.32$ Hz, 8H, $-\text{CH}_2\text{COOH}$), 1.97–1.36 (m, 72H, $-\text{OCH}_2(\text{CH}_2)_9-$), -2.67 (s, 2H, -2NH). FAB-MS for $\text{C}_{92}\text{H}_{118}\text{O}_{12}\text{N}_4$: m/z calcd., 1471.9 [M] $^+$: found, 1471.8. Anal. Calcd. for $\text{C}_{92}\text{H}_{118}\text{N}_4$: C, 75.07; H, 8.08; N, 3.80. Found: C, 74.60; H, 8.09; N, 3.79.

2.3. Preparation of a porphyrin **4** monolayer

ITO electrodes (on glass, $10 \Omega \text{cm}^{-2}$) were purchased from Sanyoshinku Co. Ltd., cut into slices (ca. $0.5 \text{cm} \times 3.0 \text{cm}$), rinsed with acetone, and dried just before being soaked in a porphyrin solution. The porphyrin solution was prepared as follows: porphyrin derivative **4** and EtOH (porphyrin concentration was 1 mM) were mixed, and then EtOH solution containing 1% KOH was added to the solution until **4** was dissolved completely. An ITO electrode was immersed in the solution for 2 days at 25 °C to form a monolayer. The ITO electrode was washed with EtOH and dried under air. The monolayer of **4** on the ITO electrode surface was characterized by cyclic voltammetry and UV–vis spectroscopy.

2.4. Spectroscopic measurements

2.4.1. Electrochemical measurements

Electrochemical measurements of **4** in solution ($c=2.6 \times 10^{-4}$ M) and of the monolayer deposited on the ITO electrode were carried out by cyclic voltammetry using a CV50W voltammetric analyzer (Version 2.0) (BAS Inc., Tokyo, Japan). Voltammetric studies were performed under a nitrogen atmosphere using a conventional three-electrode cell. The working electrode was a Pt disk (diameter 1.8 mm) for solution of **4**. A Pt wire and an Ag/AgPF₆ were the counter and reference electrodes, respectively. All potentials are referenced to Ag/AgPF₆.

2.4.2. Absorption, excitation, and emission spectroscopy

The UV–vis absorption spectra of **4** dissolved in THF ($c=2.4 \times 10^{-6}$ M) and of the monolayer on an ITO electrode were recorded using a V-570 UV–vis/NIR spectrophotometer (JASCO International Co. Ltd., Tokyo, Japan). The steady-state emission and excitation spectra of **4** dissolved in THF ($c=2.1 \times 10^{-6}$ M) were measured on a RF-5300PC spectrofluorophotometer (Shimadzu Corporation, Kyoto, Japan). A 150 W xenon lamp with a cut filter of 450 nm, Toshiba UV cut filter V-Y 45 (Toshiba, Tokyo, Japan), was used as a visible emission light source. The excitation and emission band pass widths were 3 nm.

2.5. Oxygen quenching behaviour

2.5.1. Oxygen quenching behaviour for porphyrin **4** on an ITO electrode

The oxygen quenching behaviour of **4** on an ITO electrode were studied by using a Shimadzu RF-5300PC spectrofluorophotometer with a 150 W xenon lamp source equipped with a cut filter of 390 nm, Toshiba UV cut filter V-Y 39, as a visible excitation light source. An ITO plate modified with **4** (ca. 13 mm × 30 mm) was placed diagonally relative to the quartz cell and was exposed to gas mixtures containing various concentrations of oxygen (in the range of 0–100%) produced by controlling the flow rates of oxygen and argon gases with a gas flow meter, Kofloc M₁N₁-GASCOM (Kojima Instrument Inc., Tokyo, Japan). The oxygen concentration was calculated by dividing the oxygen flow rate by the total flow rate of the mixed gases. The total pressure was maintained at 101,333 Pa (760 Torr) and all experiments were carried out at room temperature. The excitation and emission band pass widths were 5 nm. The oxygen quenching behaviour of a porphyrin **4** monolayer on the ITO electrode were characterized by the Stern–Volmer quenching constant, K_{SV} , obtained from Eq. (1):

$$\frac{I_0}{I} = 1 + K_{SV}[\text{O}_2] \quad (1)$$

where I_0 is the luminescence intensity in the absence of oxygen, I is the intensity in the presence of oxygen and $[\text{O}_2]$ is the oxygen concentration in percentage [19,20].

2.5.2. Dynamic response of oxygen quenching for porphyrin **4** on an ITO electrode

Dynamic response of oxygen quenching of the porphyrin **4** on an ITO electrode were detected conventionally with a spectrofluorophotometer, while the gas flow was switched between 100% oxygen and 100% argon using a gas flow meter, Kofloc M₁N₁-GASCOM [9]. All experiments were carried out at 101,333 Pa (760 Torr) and at room temperature.

3. Results and discussion

3.1. Electrochemical properties of the ITO electrode modified with porphyrin **4**

The redox properties of **4** deposited on an ITO electrode were characterized by cyclic voltammetry. Figs. 1 and 2 show the cyclic voltammograms of **4** in THF and **4** on an ITO electrode at different potential scan rates, respectively. As shown in Fig. 1, the cyclic voltammogram displayed characteristic features of a diffusion-controlled redox couple with the half-wave potential of 753 mV. The ratio of the re-reduction peak current to the oxidation peak current, i_{pc}/i_{pa} , is less than unity and increases with the scan rate, indicating the instability of the oxidation product in THF solution. For **4** deposited as a monolayer on an ITO electrode, repro-

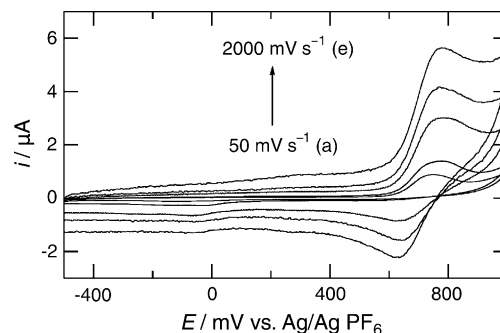


Fig. 1. Cyclic voltammograms of **4** in THF containing 0.1 M Bu₄NPF₆ as an electrolyte at scan rates of (a) 50 mV s⁻¹, (b) 100 mV s⁻¹, (c) 500 mV s⁻¹, (d) 1000 mV s⁻¹ and (e) 2000 mV s⁻¹.

ducible cyclic voltammograms were obtained after multiple scan cycles (as shown in Fig. 2). A significant symmetrical oxidation peak, corresponding to the one-electron oxidation of the porphyrin moiety, is observed at 792 mV. On the reverse scan, three re-reduction peaks appear at 3, 239 and 714 mV. The sum of these reduction peak areas is almost the same as the area of the main oxidation peak. This suggests the presence of three different adsorption states of the oxidation species, which have the possible redox centre of porphyrin moiety, in the monolayer on the ITO electrode. The peak current of the main oxidation peak increases linearly with increase of the potential scan rate, as expected from Eq. (2), which was derived for adsorbed redox species:

$$i_p = \frac{n^2 \Gamma F^2 v}{4RT} \quad (2)$$

where i_p , n , Γ , F and v are the peak current, the number of electrons, the surface coverage, the Faraday constant and the potential scan rate, respectively (Fig. 3) [21]. The charge required for the complete oxidation of **4** adsorbed on an ITO electrode, measured from the peak area, gives the surface coverage (Γ) of 2.3×10^{-10} mol cm⁻² when n is equal to 1. Furthermore, the Γ values of three samples fell in the narrow range from 2.3×10^{-10} to 2.5×10^{-10} mol cm⁻². The simple deposition method using the porphyrin with four carboxyl

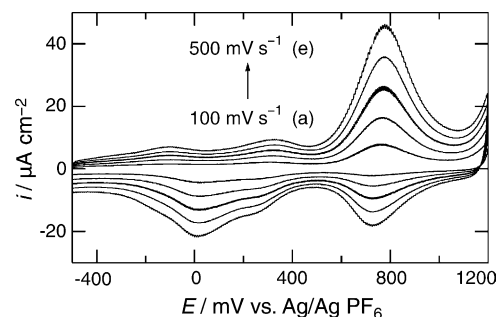


Fig. 2. Cyclic voltammograms of an ITO electrode modified with **4** in CH₃CN containing 0.1 M Bu₄NPF₆ as an electrolyte at scan rates of (a) 100 mV s⁻¹, (b) 200 mV s⁻¹, (c) 300 mV s⁻¹, (d) 400 mV s⁻¹ and (e) 500 mV s⁻¹.

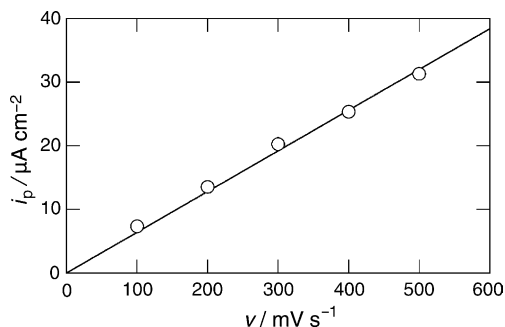


Fig. 3. Dependence of the peak current (i_p) on the potential scan rate (v) for a monolayer of **4** on an ITO electrode. Peak current was calculated from the cyclic voltammograms.

groups leads to effective and reproducible modification of the monolayer on the ITO electrode.

3.2. Optical properties of the ITO electrode modified with porphyrin **4**

Fig. 4 shows the UV–vis absorption spectra of **4** dissolved in THF and **4** on an ITO electrode in air, in the transmission mode. The Soret band of **4** on the ITO electrode (Soret band at 435.5 nm and four Q-bands at 523.0, 561.0, 599.0 and 654.5 nm) is broadened and red shifted by 15 nm relative to that in THF solution (Soret band at 420.0 nm and four Q-bands at 520.0, 553.5, 594.5 and 651.5 nm). Also, similar broadening and red shift were reported for porphyrin SAMs on gold electrodes, LB monolayers of porphyrins on glass or semiconductors and porphyrin aggregates in solutions [1,14,22–24]. A stacked face-to-face porphyrin π -aggregation (sandwich-type, *H*-aggregate) leads to a blue shift, while side-by-side porphyrin π -aggregation (*J*-aggregate) leads to a red shift [24]. Thus, the observed spectral change is due to partially *J*-aggregate like stacked structure of the porphyrins in the monolayer microenvironment.

Also, the surface coverage of the monolayer was evaluated from the absorption spectrum on the basis of Eq. (3), which is Lambert–Beer’s law modified for two-dimensional

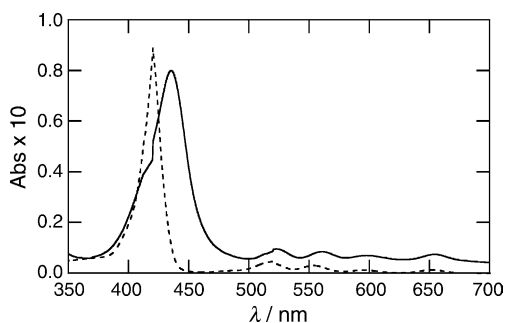


Fig. 4. UV–vis absorption spectra of **4** in THF (broken line) and on an ITO electrode (solid line).

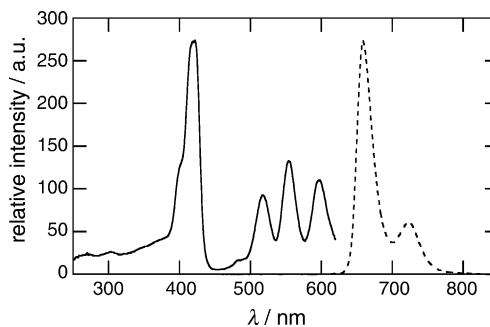


Fig. 5. Excitation (solid line) and emission spectra (broken line) of **4** in THF. $\lambda_{em} = 658$ and $\lambda_{ex} = 422$ nm were used for excitation and emission, respectively.

concentration:

$$\Gamma = \frac{10^{-3} A}{\varepsilon} \quad (3)$$

where Γ , A and ε are the surface coverage, absorbance of the monolayer and molar absorption coefficient, respectively [25,26]. Using Eq. (3), the surface coverage (Γ) of **4** deposited on the ITO electrode is calculated to be 2.19×10^{-10} mol cm $^{-2}$. This value is consistent with that derived from cyclic voltammetry. Therefore, the redox number of electrons for **4** on an ITO electrode was estimated to be 1. The luminescence of porphyrin **4** dissolved in THF ($c = 2.1 \times 10^{-6}$ M) was observed at 658 and 722 nm, on irradiation at 422 nm (Soret band), as shown in Fig. 5.

3.3. Structure of the porphyrin **4** monolayer

Fig. 6 shows possible models of **4** immobilized on an ITO electrode. In model A, the macrocyclic plane of **4** is almost perpendicular to the ITO surface, and the projection area of a molecule **4** is calculated at ca. 58 \AA^2 . In contrast, if the plane of **4** is parallel to the electrode surface, it would cover the area of 174 \AA^2 per molecule. These occupied areas of molecules lead to a maximum surface coverage of **4** of 2.9×10^{-10} mol cm $^{-2}$ for model A and of 9.5×10^{-11} mol cm $^{-2}$ for model B. The surface coverage of the perpendicular model of 2.9×10^{-11}

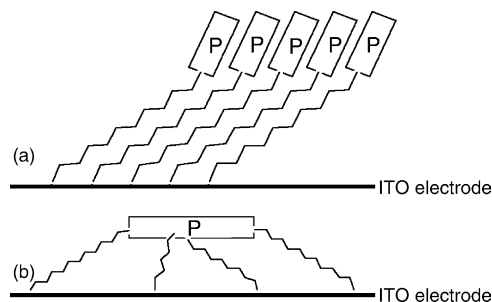


Fig. 6. Possible structures of a monolayer of **4** immobilized on an ITO electrode in which one or two carboxylic groups bind to the surface (model A, loose binding model) or four carboxylic groups bind to the surface (model B, tight binding model) (P, porphyrin core).

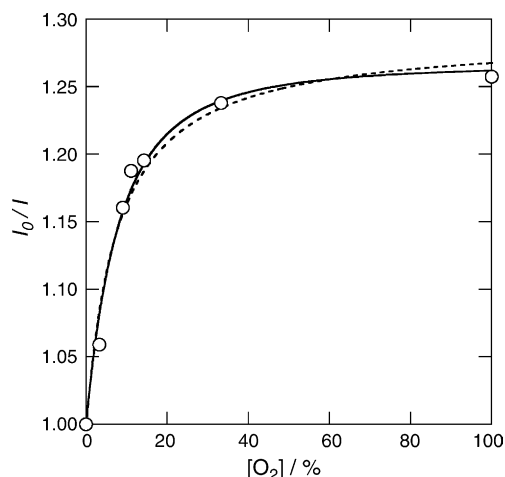


Fig. 7. Stern–Volmer plot for **4** immobilized on an ITO electrode. (Broken line; $K_{SV1} = 0.170\%^{-1}$, $K_{SV2} = 0\%^{-1}$ and $f_1 = 0.224$. Solid line; K_{SV1} and $K_{eq} = 0.073$ and $0.078\%^{-1}$, $K_{SV2} = 0\%^{-1}$ and $f_1 = 0.210$).

mol cm^{-2} is almost the same as the surface coverage of $(2.3\text{--}2.5) \times 10^{-10} \text{ mol cm}^{-2}$ estimated from the cyclic voltammogram. Hence, the major binding structure of **4** should be that shown in model A.

3.4. Oxygen quenching behaviour of the porphyrin **4** monolayer on an ITO electrode

Fig. 7 shows the intensity changes of the luminescence from a monolayer of **4** as a function of oxygen concentration. The oxygen quenching ratio of the monolayer was $I_0/I_{100} = 1.25$, where I_0 and I_{100} are the luminescence intensity in the absence and in the presence of oxygen, respectively. While the resulting plot shows considerable linearity at lower oxygen concentration, non-linearity is observed at higher oxygen concentration. Such behaviour can be attributed to heterogeneity of the quenching sites of the sensing component; each type of site has its own Stern–Volmer constant. In general, the observed plots fit very well to a two-site quenching model described by the following modified Stern–Volmer Eq. (4):

$$\frac{I_0}{I} = \frac{1}{f_1/(1 + K_{SV1}[O_2]) + (1 - f_1)/(1 + K_{SV2}[O_2])} \quad (4)$$

where f_1 is the fractional intensity contribution of the component of the Stern–Volmer constant K_{SV1} in the absence of oxygen [12,27,28]. In our system, curve fitting to Eq. (4) gave the parameters $K_{SV1} = 0.121\%^{-1}$, $K_{SV2} = -0.000513\%^{-1}$ and $f_1 = 0.263$. The Stern–Volmer constant must be positive and K_{SV2} is negligibly small and can be regarded as zero, Eq. (4) can be modified to yield Eq. (5).

$$\frac{I_0}{I} = \frac{1}{f_1/(1 + K_{SV1}[O_2]) + (1 - f_1)} \quad (5)$$

Curve fitting to Eq. (5) gave the parameters $K_{SV1} = 0.170\%^{-1}$ and $f_1 = 0.224$ (broken line, Fig. 7). Eq. (5) reproduces the non-linearity of the plot well. However, there is still significant deviation from observation in the higher oxygen concentration region, where the observed luminescence intensity from the monolayer of **4** is lower than that predicted by Eq. (5). In order to explain this phenomenon, we take into account adsorbed oxygen molecules on the monolayer. The adsorption equilibrium is defined by Eq. (6):

$$K_{eq} = \frac{[MO_2]}{[M][O_2]} = \frac{[M]_0 - [M]}{[M][O_2]} \quad (6)$$

where K_{eq} , $[MO_2]$, $[M]$ and $[M]_0$ are the equilibrium constant, the amount of dye statically quenched by oxygen molecules, the amount of free dye and the total amount of dye, respectively. In this scheme, the dye in the MO_2 region is no longer available for oxygen quenching. Hence, Eq. (6) is modified as follows.

$$\frac{I_0}{I} = \frac{1}{\phi f_1/(1 + K_{SV1}[O_2]) + (1 - f_1)} \quad (7)$$

$$\phi = \frac{[M]}{[M]_0} = \frac{1}{1 + K_{eq}[O_2]} \quad (8)$$

The result of curve fitting to Eq. (7) is shown in Fig. 8 as a solid line. The parameter f_1 is equal to 0.210 and values of 0.073 and $0.078\%^{-1}$ are obtained for K_{SV1} and K_{eq} . In Eq. (7), the two parameters K_{SV1} and K_{eq} are identical mathematically, so it is impossible to assign them individually. The term ϕ , improves the fitting to the plots (solid line, Fig. 7), suggesting an influence of adsorbed oxygen molecules. Even though the Stern–Volmer plot of the monolayer shows the significant non-linearity, the modified two-site quenching model represents the oxygen sensing properties well. Hence, the monolayer of porphyrin derivatives **4** is an ultra thin film capable of oxygen sensing.

3.5. Dynamic oxygen quenching behaviour for the porphyrin **4** monolayer on an ITO electrode

Fig. 8 shows a typical dynamic response of the oxygen quenching when 100% oxygen and 100% argon gases were

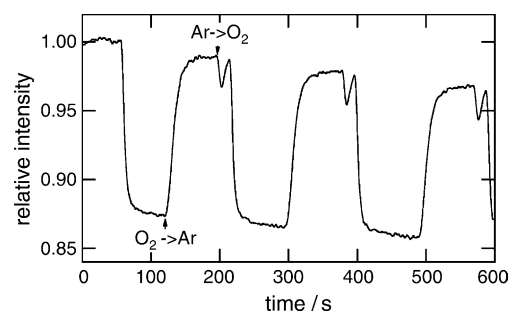


Fig. 8. Dynamic response times for **4** immobilized on an ITO electrode. (Response times were 10 and 23 s, respectively.)

switched for 600 s. The response times for luminescence quenching are defined as the times taken to reach the 90% of the ultimate response. The response times of the porphyrin **4** monolayer onto ITO electrode are 10 s on going from argon to oxygen and 23 s on going from oxygen to argon. As shown in Fig. 8, a large noise signal (indicated by an arrow) is observed; this is caused by the non-ideal behaviour of the gas-switching mechanism used to purge the sample container.

4. Conclusion

A porphyrin with long alkyl chains **4** was synthesized and immobilized on an ITO electrode using a dipping method. Cyclic voltammetry indicated that the immobilization was successful and showed fairly good reproducibility. Furthermore, the UV–vis absorption spectrum of the monolayer of **4** on the ITO electrode indicated the presence of *J*-aggregate like partially stacked structures. The major binding structure of **4** on the electrode was a perpendicular one in which one or two carboxylic groups bind to the surface. A monolayer of **4** on an ITO electrode was tested for oxygen quenching ability. For the luminescence quenching ability by oxygen gas of the porphyrin **4** monolayer, the Stern–Volmer quenching coefficient (K_{SV}) and the equilibrium constant (K_{eq}), were 0.073 and $0.078\%^{-1}$, these two parameters are impossible to distinguish. The response times for the porphyrin **4** monolayer were 10 s on going from argon to oxygen and 23 s on going from oxygen to argon. This is the first time that a monolayer has been studied for a luminescence quenching by oxygen gas.

A precise reduced scale model coated with luminescence dye is used in wind tunnel experiment based on oxygen-induced luminescence quenching mechanism, for aircraft and rockets [29]. In this technology, the coating deteriorates the size-accuracy of the model, even though the thickness is the order of a few micrometer. In this point of view, the monolayer of sensing dye, which has thickness of the order of a few nanometer, is the ultimate sensing system for keeping the size-accuracy of the model. The coatings of well-packed dyes are thought to be useless for oxygen sensing because of luminescence quenching by the self-aggregation of chromophores. However, the results presented indicate that a porphyrin monolayer emits a luminescence and can be applicable for oxygen sensing. In order to improve sensing properties, the sensing monolayer using metalloporphyrins and other luminescence dye is under investigation.

Acknowledgements

This work was supported by Grants-in-Aid for Scientific Research on Priority Areas (417, 434) and 13557211,

15033246, 16350032, 17029040 and 17036041 from the Ministry of Education, Culture, Sports, Science and Technology (MEXT) of the Japanese Government, and grants from Osaka Gas and San-EiGen Foundation for chemical research, and also in part by Special Coordination Funds for ‘Molecular Sensors for Aero-Thermodynamic Research (MOSAIC)’ from the Ministry of Education, Culture, Sports, and Science and the Technology Agency.

References

- [1] H. Imahori, H. Yamada, Y. Nishimura, I. Yamazaki, Y. Sakata, *J. Phys. Chem. B* 104 (2000) 2099.
- [2] D.J. Campbell, B.R. Herr, J.C. Hulteen, R.P. Van Duyne, C.A. Mirkin, *J. Am. Chem. Soc.* 118 (1996) 10211.
- [3] H. Imahori, Y. Kashiwagi, T. Hasobe, M. Kimura, T. Hanada, Y. Nishimura, I. Yamazaki, Y. Araki, O. Ito, S. Fukuzumi, *Thin Solid Film* 451–452 (2004) 580.
- [4] H. Imahori, M. Arimura, T. Hanada, Y. Nishimura, I. Yamazaki, Y. Sakata, S. Fukuzumi, *J. Am. Chem. Soc.* 1123 (2001) 335.
- [5] K. Uosaki, T. Kondo, X. Zhang, M. Yanagida, *J. Am. Chem. Soc.* 119 (1997) 8367.
- [6] D.A. Offord, S.B. Sachs, M.S. Ennis, T.A. Eberspacher, J.H. Griffin, C.E.D. Chidsey, J.P. Collman, *J. Am. Chem. Soc.* 120 (1998) 4478.
- [7] A.A. Yasseri, D. Syomin, V.L. Malinovskii, R.S. Loewe, J.S. Lindsey, F. Zaera, D.F. Bocian, *J. Am. Chem. Soc.* 126 (2004) 11944.
- [8] Y. Amao, K. Asai, I. Okura, H. Shinohara, H. Nishide, *Analyst* 125 (2000) 1911.
- [9] Y. Amao, K. Miyakawa, I. Okura, *J. Mater. Chem.* 10 (2000) 305.
- [10] S. Lee, I. Okura, *Anal. Commun.* 34 (1997) 185.
- [11] S. Lee, I. Okura, *Analyst* 122 (1997) 81.
- [12] Y. Amao, I. Okura, *Analyst* 125 (2000) 1601.
- [13] H. Imahori, Y. Mori, Y. Matano, *J. Photochem. Photobiol. C* 4 (2003) 51.
- [14] H. Imahori, H. Norieda, Y. Nishimura, I. Yamazaki, K. Higuchi, N. Kato, T. Motohiro, H. Yamada, K. Tamaki, M. Arimura, Y. Sakata, *J. Phys. Chem. B* 104 (2000) 1253.
- [15] A. Ulman, *Chem. Rev.* 96 (1996) 1533.
- [16] Z. Zhang, N. Yoshida, T. Imae, Q. Xue, M. Bai, J. Jiang, Z. Liu, *J. Colloid Interface Sci.* 243 (2001) 382.
- [17] Z. Zhang, T. Imae, *Nano Lett.* 5 (2001) 241.
- [18] M.M. Walczak, C. Chung, S.M. Stole, C.A. Widrig, M.D. Porter, *J. Am. Chem. Soc.* 113 (1991) 2370.
- [19] E.R. Carraway, J.N. Demas, B.A. DeGraff, *Anal. Chem.* 63 (1991) 332.
- [20] J. Olmsted III, *Chem. Phys. Lett.* 26 (1974) 33.
- [21] A.J. Bard, L.R. Faulkner, *Electrochemical Methods Fundamentals and Applications*, Wiley, New York, 2001 (chapter 14).
- [22] R.F. Khairutdinov, N. Serpone, *J. Phys. Chem. B* 103 (1999) 761.
- [23] D.L. Akins, S. Özçelik, H. Zhu, C. Guo, *J. Phys. Chem. B* 100 (1996) 14390.
- [24] A. Ishida, T. Majima, *Chem. Commun.* 14 (1999) 1299.
- [25] T. Taniguchi, Y. Fukasawa, T. Miyashita, *J. Phys. Chem. B* 103 (1999) 1920.
- [26] B.W. Chu, V.W. Yam, *Inorg. Chem.* 49 (2001) 3324.
- [27] A. Mills, M.D. Thomas, *Analyst* 123 (1998) 1135.
- [28] Y. Fujiwara, Y. Amao, *Sens. Actuators B* 89 (2003) 187.
- [29] M. Gouterman, B. Idea, *J. Chem. Educ.* 74 (1997) 697.